

REE geochemistry of Early Cambrian phosphorites from Gezhongwu Formation at Zhijin, Guizhou Province, China*

SHI Chunhua (施春华)^{1,2} and HU Ruizhong (胡瑞忠)¹

¹ Key Laboratory of Ore Deposit Geochemistry, Institute of Geochemistry, Chinese Academy of Sciences, Guiyang 550002, China

² Graduate School, Chinese Academy of Sciences, Beijing 100039, China

Abstract The Cambrian Gezhongwu Formation in Southwest China is the lowest Cambrian phosphorite unit. The Formation belongs to the Meishucun stage with small shelly fossils. Rare-earth element (REE) data from the Gezhongwu phosphorites of Zhijin documented the depositional conditions. The total REE concentrations are high in the Gezhongwu phosphorites, which are especially rich in yttrium. The PAAS-normalized REE patterns of the Gezhongwu phosphorites are characterized by negative Ce anomalies and slight enrichment of MREE, as being hat-shaped. The hat-shaped patterns suggest that the REE originated from depositional environments rather than from subsequent diagenesis. The negative Ce anomalies indicate that the depositional environments are oxic. The positive Eu anomaly, the high total REE and the hat-shaped REE pattern revealed contributions from the normal marine environment mixed with hydrothermal water to the REE budget of the Gezhongwu phosphorites.

Key words phosphorite; Cambrian; REE; Guizhou Province

1 Introduction

Marine biogenic phosphorite is regarded as one of the main suitable rocks to decipher the geochemical signatures (e. g. REE contents, REE patterns, and Ce anomalies) of marine depositional environments (Wright et al., 1987; Grandjean et al., 1987; Bertram et al., 1992; Ilyin, 1998; Yang Jiedong and Sun Weiguo, 1999; Mazumdar et al., 1999; Chen Duofu et al., 2003). Phosphorites commonly display highly variable REE patterns (Jarvis et al., 1994; Shields and Stille, 2001) due to variations in the composition and amount of associated detritus, depositional environment, sea- and pore-water redox, pH, age, and water depth (German and Elderfield, 1990; Jarvis et al., 1994; Bertrand et al., 1997; Hannigan and Sholkovitz, 2001; Picard et al., 2002). However, REE signatures may be modified by burial diagenesis (Elderfield and Sholkovitz, 1987; German and Elderfield, 1990; Murray et al., 1992; Reynard et al., 1999; Shields and Stille, 2001; Yang Yaomin et al., 2004), or by surface weathering (McArthur and Walsh, 1984; Bonnoit and Flicoteaux, 1989; Hannigan and Sholkovitz, 2001). Therefore, there is a con-

siderable uncertainty about whether the REE from marine phosphorites can be used as a reliable indicator of seawater composition.

One of the most important global phosphogenesis events took place at the Precambrian-Cambrian boundary. Such event is attributed to oceanic turnover that resulted in transgression of nutrient-rich, anoxic waters onto continental shelves (Cook and Shergold, 1984). The Gezhongwu Formation in Guizhou is the lowest unit of Cambrian, Meishucunian in age. Phosphorites from this formation are REE-rich. This paper dealt with the REE geochemistry of the Gezhongwu phosphorites.

2 Geological setting and sampling

The Gezhongwu section is located in the Gezhongwu phosphorite mine in the eastern part of Zhijin County, Guizhou Province, Southwest China (Fig. 1). The Gezhongwu phosphorite beds belong to the Meishucun stage, and are distributed in the southwest of the central Guizhou uplift, Yangtze block. This region is dominated by normal faults with local small-scale drapes. The Gezhongwu Formation is a major phosphorite-producing layer with a maximum thickness of 22 m. It conformably rests on the Sinian dolomites of the Dengying Formation, and is overlain by the Early Cambrian black carbonaceous shales of the Niutitang Formation, consisting mainly of Y-rich bioclastic dolomitic and siliceous phosphorites.

The dolomitic and siliceous phosphorites alternate with phosphoritic bioclastic dolomite, resulting in lenticular, wavy and chevron cross-beddings. The phosphate rock consists mainly of francolite, which is amorphous, aphanitic and gelatinous as replacements of bioclast and intraclast. Twelve phosphorite samples were collected from the Gezhongwu section. Detailed petrographical description and sample localities are shown in Fig. 2.

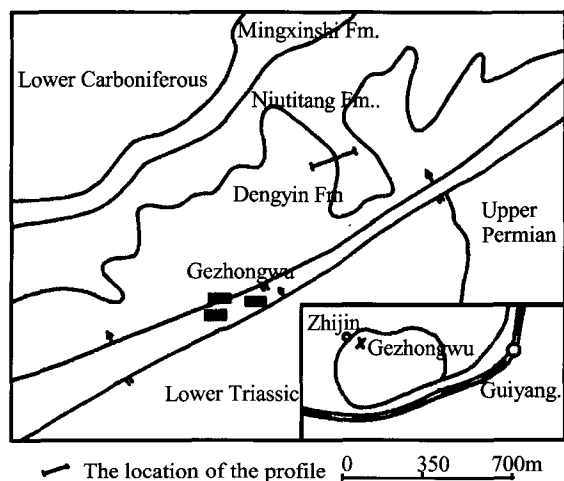


Fig. 1. Geological sketch map and sample localities in the Zhijin area.

3 Analytical methods

Fresh samples were carefully prepared before crushing. Fine-grained material was sorted under binocular microscope to obtain pure samples. Grains, from 60 to 80 mesh in size, were selected and thoroughly cleaned in an ultrasonic bath using double-distilled deionized water and dried at 100°C for several hours. Subsequently, the samples were milled as fine as less than 200-mesh. One hundred milligrams of powdered sample were digested with 1 mL of HF (38%) and 0.5 mL of HNO₃ (68%) in screw top PTFE-lined stainless steel bombs at 190°C for more than 12 hours. The solution was then drained and evaporated till dryness with 0.5 mL HNO₃ (repeated two times). The final residue was redissolved by adding 6 mL of 40% HNO₃, followed by resealing the bombs and getting them heated again over the electric oven at 140°C for 3 hours. Upon cooling, each final solution was diluted to 100 mL by adding distilled deionized water. The reagent blanks were treated exactly as the samples. Analytical reagent-grade HF and HNO₃ were used and purified prior to use by sub-boiling distillation. The PTFE bombs were cleaned with 20% HNO₃ (volume/volume) heated to 110°C for 1 hour.

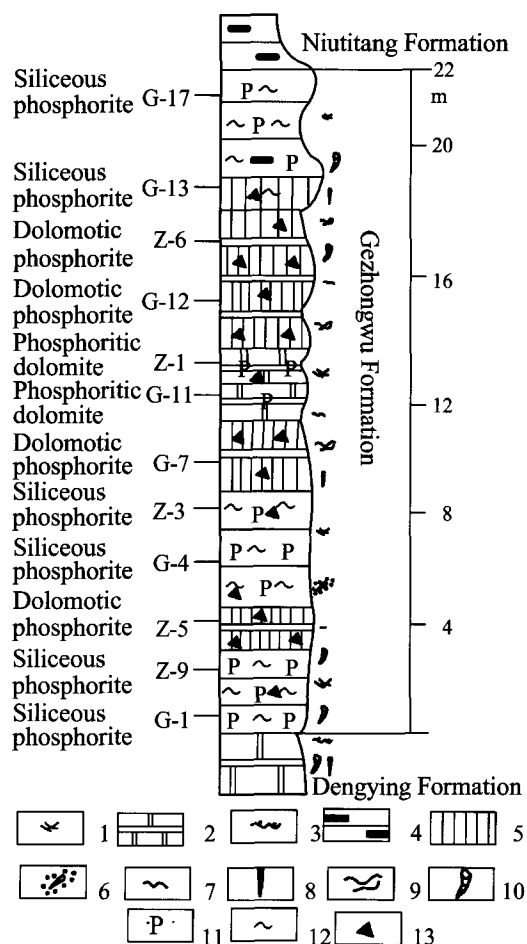


Fig. 2. Integrated stratigraphical column of the Gezhongwu section, showing the positions and features of samples. 1. Chevron cross-bedding; 2. dolomite; 3. wash; 4. black carbonaceous shale; 5. phosphorite; 6. small shelly fossil; 7. undulated lamina; 8. spicula; 9. ripple biscuit; 10. Hyolitha fossil; 11. phosphoritic rock; 12. siliceous rock; 13. biotritus.

The REE were analyzed by Finnigan Mat Element high resolution ICP-MS at the Key Laboratory of Ore Deposits, Chinese Academy of Sciences, Guiyang, China. All instrumental operating parameters are referenced in Qi Liang and Gregoire (2000). To guarantee the quality of the data, we analyzed standards GBPG-1 of GeoPT7 and AMH-1 of GeoPT5 (an international proficiency test for analytical geochemistry laboratories). The precision was checked by multiple analyses of standard samples GBPG-1 and AMH-1.

Data from 14 analyses are listed in Table 1. The average standard deviations are less than 10%, and the average relative standard deviations are better than 5% for Y and REE. The accuracy is checked by comparing our ICP-MS data with the standard reference data and two internal reference samples of DBS-12 material in-

cluded in Table 1. The data fit well with the standard DBS-12 material without systematic bias. data and between two internal reference samples of

Table 1. Abundances of REE, Y and Zr in standards GBPG-1 and AMH-1 and internal reference sample DBS-12 determined in this study ($\times 10^{-6}$)

| | GBPG-1 | | | AMH-1 | | | | DBS-12 | |
|----|--------|--------|--------|-------|--------|--------|-------|--------|-------|
| | R | A | b | R | a | b | c | a | b |
| La | 52.95 | 51.47 | 51.18 | 15.87 | 15.69 | 16.06 | 15.72 | 11.8 | 11.26 |
| Ce | 103.2 | 104.23 | 101.66 | 33.03 | 33.41 | 34.73 | 32.68 | 15.97 | 14.6 |
| Pr | 11.45 | 11.25 | 11.11 | 4.21 | 4.04 | 4.05 | 4.34 | 2.84 | 2.67 |
| Nd | 43.3 | 42.27 | 41.15 | 17.69 | 16.61 | 16.81 | 18.15 | 13.62 | 13.34 |
| Sm | 6.79 | 6.88 | 6.644 | 3.68 | 3.89 | 3.78 | 3.85 | 3.35 | 3.34 |
| Eu | 1.79 | 1.67 | 1.68 | 1.16 | 1.04 | 1.05 | 1.16 | 0.88 | 0.86 |
| Gd | 4.74 | 4.52 | 4.51 | 3.34 | 3.31 | 3.09 | 3.57 | 4.68 | 4.33 |
| Tb | 0.6 | 0.59 | 0.6 | 0.51 | 0.5 | 0.52 | 0.52 | 0.71 | 0.68 |
| Dy | 3.26 | 3.06 | 3.26 | 2.84 | 2.92 | 2.83 | 3.02 | 4.16 | 4.07 |
| Ho | 0.69 | 0.64 | 0.63 | 0.57 | 0.55 | 0.58 | 0.59 | 0.93 | 0.93 |
| Er | 2.01 | 1.93 | 1.98 | 1.52 | 1.52 | 1.53 | 1.61 | 2.38 | 2.45 |
| Tm | 0.3 | 0.31 | 0.29 | 0.21 | 0.21 | 0.23 | 0.22 | 0.32 | 0.29 |
| Yb | 2.03 | 2.1 | 2.11 | 1.37 | 1.41 | 1.45 | 1.41 | 1.67 | 1.65 |
| Lu | 0.31 | 0.29 | 0.3 | 0.21 | 0.23 | 0.19 | 0.21 | 0.22 | 0.21 |
| Y | 18 | 17.53 | 18.27 | 16.44 | 15.57 | 16.23 | 16.59 | 29.86 | 40.49 |
| Zr | 231.8 | 219.99 | 251.22 | 146 | 143.39 | 145.53 | 145.2 | 9.5 | 8.61 |

Note: R. Reference data of GBPG-1 and AMH-1 are obtained from round 7, GeoPT7 and PT5 (an international proficiency test for analytical geochemistry laboratories), respectively, a, b in GBPG-1 (two copies), a, b, c in AMH-1 (three copies), and a and b in DBS-12 (two copies); this study, average of 14 in which standard deviations (1σ) are less than 10%; average relative standard deviations are better than 5%.

In this paper, Ce/Ce^* denotes $Ce_N/(La_N \times Pr_N)^{0.5}$; Eu/Eu^* , $Eu_N/(Sm_N \times Gd_N)^{0.5}$; and Pr/Pr^* , $Pr_N/(Ce_N \times Nd_N)^{0.5}$, where N refers to the normalization of concentrations against the standard post-Archean Australian Shale (McLennan, 1989).

4 Results and discussion

4.1 REE concentrations

The total REE concentrations range from 412.55×10^{-6} to 1059.59×10^{-6} in the siliceous and dolomitic phosphorites, from 242.92×10^{-6} to 384.14×10^{-6} in the phosphatic dolomites. The two types of sample are all chemically sedimentary rocks, but differ in way of their incorporation with the REE. Dolomite is perfect in crystal structure. As Mg ions are different in ionic radius from REE, dolomites are exclusive to the latter. Phosphorite consists of francolite, which is of open-hexagonal prism and Ca resembles REE in ionic radius, REE may be incorporated into phosphorites by isomorphous replacement. This is the main reason why phosphorite is rich in REE. Contrast with the published data, these analyzed values are higher than those of the Early Cambrian phosphorites (46.63×10^{-6} – 332.63×10^{-6}) from the east of Yunnan (Yang Weidong and Qi Liang, 1995). They are in the range of 'old' (Vendian-Early Cambrian) phosphor-

ites (Ilyin, 1998), close to the world-average of 700×10^{-6} (Altschuler, 1980). These coincide with the results obtained by Li Shengrong and Gao Zhenmin (1995), i. e., the ΣREE is high in normal sea-water sediments.

Yttrium (114.90×10^{-6} – 387.09×10^{-6}) is markedly enriched in the Gezhongwu phosphorites relative to average shales (27×10^{-6} in PAAS). Its overall concentrations are comparable to the global average of phosphorites (40×10^{-6} – 610×10^{-6} ; Altschuler, 1980). The observed Y enrichment is possibly due to a preferential uptake of Y relative to other lanthanides.

The HREE concentrations of the Gezhongwu phosphorites ($\Sigma HREE 37.4 \times 10^{-6}$ to 169.2×10^{-6}) are distinctly higher than those of shales (17.5×10^{-6} in PAAS), but the values are much lower than the LREE concentrations (205.6×10^{-6} to 890.4×10^{-6}) of the Gezhongwu phosphorites. Very low concentrations of Zr (7.9×10^{-6} to 26.78×10^{-6}) and HREEs vs. Zr correlation factor ($r = 0.2$) suggest that the detrital zircon fraction contributed little to the HREEs. Although zircons were not dissolved completely, REE analysis is permitted. Consequently, HREE depletion in the francolite phase resulted in the HREE-depleted patterns in some phosphorite samples. Similar HREE depletion was reported by Ilyin (1998) for many 'old' Asian phosphorites.

Table 2. REE, Y and Zr contents of the Gezhongwu phosphorites ($\times 10^{-6}$)

| Sample No. | G-1 | G-4 | G-7 | G-11 | G-12 | G-13 | G-17 | Z-1 | Z-3 | Z-5 | Z-6 | Z-9 |
|----------------------------------|--------|--------|--------|--------|--------|--------|--------|-------|--------|--------|--------|--------|
| La | 157.01 | 241.06 | 160.46 | 101.11 | 163.39 | 136.68 | 268.38 | 72.47 | 193.34 | 153.79 | 120.47 | 234.42 |
| Ce | 135.55 | 197.92 | 120.11 | 85.39 | 116.30 | 112.59 | 229.30 | 48.52 | 126.47 | 103.04 | 89.05 | 175.41 |
| Pr | 38.16 | 54.51 | 32.52 | 20.39 | 31.98 | 27.74 | 60.97 | 13.37 | 34.19 | 28.10 | 21.86 | 48.44 |
| Nd | 163.63 | 242.97 | 143.36 | 94.76 | 139.99 | 123.43 | 262.41 | 57.72 | 147.97 | 121.30 | 93.24 | 205.70 |
| Sm | 30.66 | 48.39 | 28.04 | 18.16 | 25.62 | 23.47 | 51.56 | 9.98 | 27.85 | 22.97 | 17.22 | 36.36 |
| Eu | 9.27 | 13.38 | 8.92 | 7.49 | 7.14 | 9.32 | 17.75 | 3.50 | 8.67 | 7.18 | 6.38 | 12.67 |
| Gd | 36.61 | 55.87 | 32.86 | 22.47 | 31.50 | 30.72 | 63.77 | 13.29 | 34.50 | 28.78 | 22.33 | 46.56 |
| Tb | 4.99 | 6.98 | 4.12 | 2.78 | 4.04 | 3.78 | 8.24 | 1.75 | 4.57 | 3.70 | 3.06 | 6.43 |
| Dy | 28.96 | 38.95 | 22.93 | 15.37 | 22.67 | 21.12 | 46.10 | 10.16 | 26.17 | 21.52 | 17.58 | 36.99 |
| Ho | 6.15 | 7.91 | 4.92 | 3.22 | 4.70 | 4.59 | 9.45 | 2.12 | 5.66 | 4.71 | 3.95 | 8.20 |
| Er | 15.49 | 20.25 | 11.98 | 8.00 | 12.11 | 11.00 | 23.95 | 5.66 | 14.75 | 11.85 | 10.29 | 21.43 |
| Tm | 1.78 | 2.26 | 1.34 | 0.86 | 1.34 | 1.23 | 2.76 | 0.68 | 1.64 | 1.35 | 1.14 | 2.43 |
| Yb | 8.40 | 10.90 | 6.24 | 3.68 | 6.06 | 5.57 | 13.17 | 3.25 | 7.59 | 6.18 | 5.37 | 11.78 |
| Lu | 1.01 | 1.30 | 0.77 | 0.46 | 0.71 | 0.66 | 1.78 | 0.47 | 0.99 | 0.79 | 0.62 | 1.39 |
| Σ REE | 637.7 | 942.6 | 578.5 | 384.1 | 567.5 | 511.9 | 1059.6 | 242.9 | 634.4 | 515.3 | 412.6 | 848.2 |
| Σ LREE | 534.3 | 798.2 | 493.4 | 327.3 | 484.4 | 433.2 | 890.4 | 205.6 | 538.5 | 436.4 | 348.2 | 713.0 |
| Σ HREE | 103.4 | 144.4 | 85.1 | 56.8 | 83.1 | 78.7 | 169.2 | 37.4 | 95.9 | 78.9 | 64.3 | 135.2 |
| Y | 285.7 | 375.8 | 238.8 | 168.5 | 247.1 | 231.5 | 361.3 | 114.9 | 292.5 | 237.4 | 212.6 | 387.1 |
| Zr | 15.27 | 19.78 | 9.25 | 15.30 | 25.83 | 24.96 | 18.70 | 7.88 | 14.85 | 12.11 | 17.80 | 26.78 |
| La _N /Sm _N | 0.74 | 0.72 | 0.83 | 0.81 | 0.93 | 0.85 | 0.76 | 1.06 | 1.01 | 0.97 | 1.02 | 0.94 |
| Ce/Ce* | 0.40 | 0.40 | 0.38 | 0.43 | 0.37 | 0.42 | 0.41 | 0.36 | 0.36 | 0.36 | 0.40 | 0.38 |
| Eu/Eu* | 1.30 | 1.21 | 1.38 | 1.75 | 1.18 | 1.63 | 1.46 | 1.43 | 1.32 | 1.32 | 1.53 | 1.45 |
| Er _N /Lu _N | 2.33 | 2.37 | 2.38 | 2.64 | 2.60 | 2.54 | 2.04 | 1.85 | 2.26 | 2.28 | 2.51 | 2.35 |
| Dy _N /Sm _N | 1.12 | 0.95 | 0.97 | 1.00 | 1.05 | 1.07 | 1.06 | 1.21 | 1.11 | 1.11 | 1.21 | 1.21 |

4.2 PAAS-normalized REE patterns

PAAS-normalized REE concentrations plotted against the respective atomic numbers are characterized by slight MREE enrichment, forming the hat-shaped REE patterns (Fig. 3). These REE patterns reflect the original seawater chemistry, differing from the convex or bell-shaped patterns that are typical of strongly altered phosphorites (Lecuyer et al., 1998; Picard et al., 2002). In addition, Barfod et al. (2002) have shown that Pb isotopic systematics in the Cambrian phosphorites also reflects depositional conditions rather than diagenetic conditions. Therefore, the REE patterns in the Cambrian phosphorites might have preserved the primary signatures of seawater.

All of the phosphorite samples show a characteristic negative Ce anomaly with variable Eu enrichment. If the Eu anomaly is ignored, all phosphorite samples will display normal seawater patterns. Europium is believed to be the only other REE, which may change its valency in the near-surface environment (Brookins, 1989), whereby Eu^{3+} may be reduced to Eu^{2+} under extremely reducing conditions. The $\text{Eu}^{3+}/\text{Eu}^{2+}$ redox potential decreases considerably under elevated temperatures (Sverjensky, 1984), with temperatures greater than 200°C being normally required for Eu^{2+} to be stable (Bau, 1991), but is less sensitive to changes in

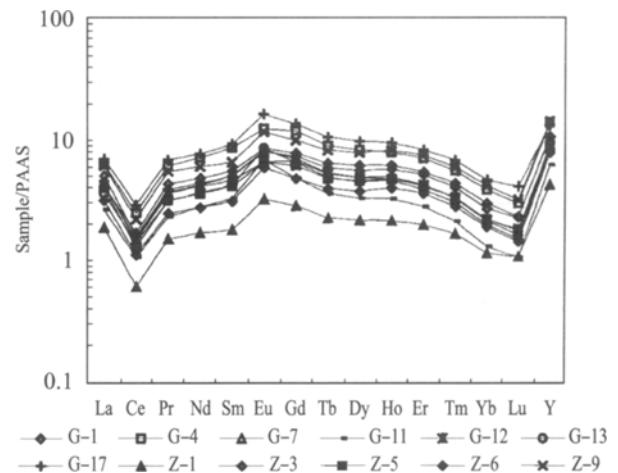


Fig. 3. PAAS-normalized REE patterns in the Gezhongwu phosphorites.

pH and pressure. Therefore, Eu is found enriched in highly reducing hydrothermal fluids (Michard and Albarède, 1986; Olivarez and Owen, 1991) and in Carich, early-magmatic minerals such as anorthosites, where Eu^{2+} may replace Sr^{2+} due to their similar ionic radii (Haskin, 1990). The common absence of anorthositic bodies in the Gezhongwu section rules out

the possibility that continental anorthosites are the source of REEs. The Gezhongwu phosphorites recorded the positive Eu anomalies ranging from 1.18 to 1.75, suggesting the REEs may originate from hydrothermal waters.

These REE plots show a relatively steep fall from Er to Lu. Similar HREE distribution patterns have been reported by Ilyin (1998) from many Precambrian-Cambrian phosphorites. Er_N/Lu_N ratios in the Gezhongwu phosphorites range from 1.85 to 2.64. These values are consistent with the ratios in Cambrian phosphorites (Er_N/Lu_N : 1.73 – 3.37), suggesting that they have not suffered from diagenetic HREE fractionation (Shields and Stille, 2001). The fact that HREE depletion is commonly observed in well-preserved samples (Shields and Stille, 2001) also suggests that the HREEs are primary rather than diagenetic.

Weathering is a factor leading to leaching of dolo-

mite and enrichment of phosphate in the Gezhongwu phosphorites. Shields and Stille (2001) suggested weathering should produce a positive correlation between La_N/Sm_N and Y/Y^* . There is no such a positive correlation observed in the Gezhongwu phosphorites (Fig. 4). Leaching experiments on phosphatic shales showed that MREE were leached preferentially over other REEs (Hannigan and Sholkovitz, 2001), suggesting that the weathered remnant samples should show MREE depletion, in other words, show enrichment in HREE and LREE. HREE depletion in the Gezhongwu phosphorites is thus unlikely the result of surface weathering.

In conclusion, the later diagenetic and weathering processes seem to have only minimally affected the REE patterns of the Gezhongwu phosphorites. The hat-shaped REE patterns seem to be primary (McArthur and Walsh, 1984; Ilyin, 1998; Lecuyer et al., 1998; Picard et al., 2002).

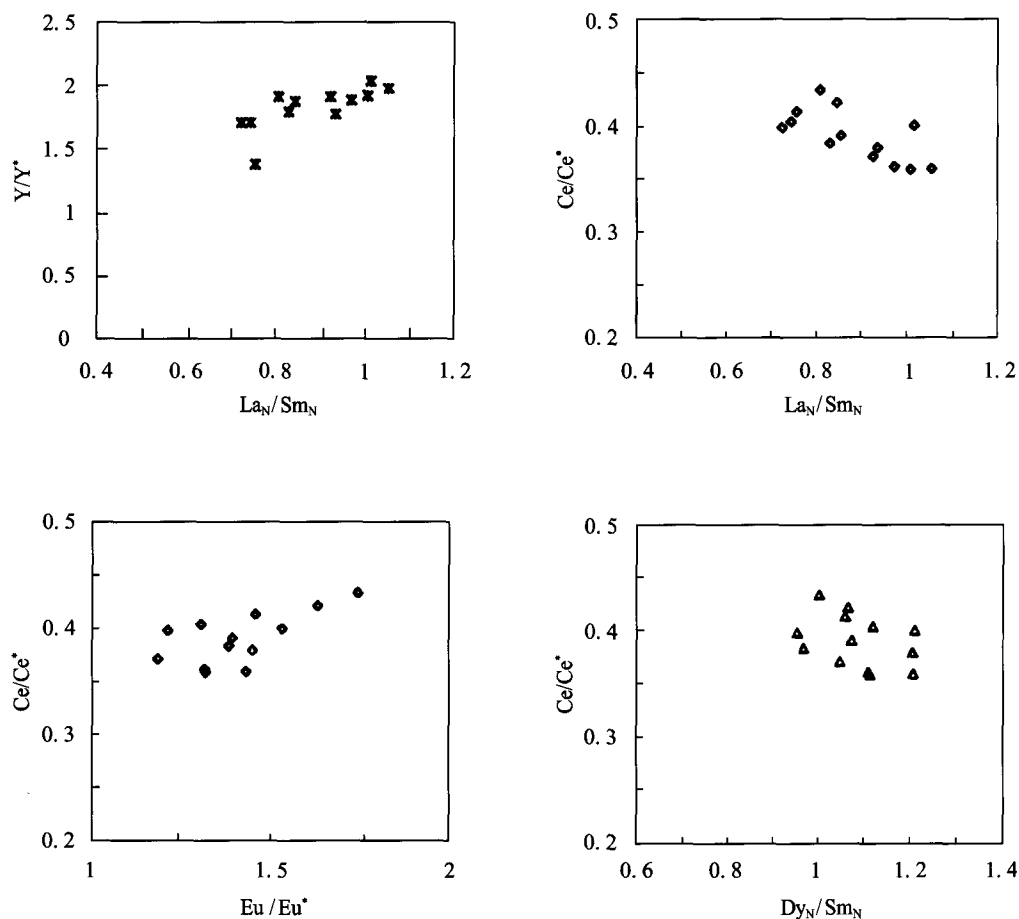


Fig. 4. Crossplots of various parameters calculated from the PAAS-normalized REE abundances of the Gezhongwu phosphorites. Plots show there is no correlation between the parameters for the PAAS-normalized REE abundances.

4.3 Ce anomaly

In the case of oxidizing conditions, Ce^{3+} may be oxidized to Ce^{4+} and then leached, resulting in a negative Ce anomaly. Negative Ce anomalies in francolites may have directly inherited from seawater under oxic condition (McArthur and Walsh, 1984). Thus, Ce anomalies (related to the other REE) have been used to infer depositional redox conditions (Wright et al., 1987; Bertram et al., 1992; Jarvis et al., 1994; Yang Jiedong and Sun Weiguo, 1999; Mazumdar et al., 1999; Shields and Stille, 2001).

Ce anomalies may be modified in later diagenesis (McArthur and Walsh, 1984; Shields and Stille, 2001). However, Morad and Felitsyn (2001) suggested that Ce anomaly in apatites represents primary signatures if there is no correlation between La_N/Sm_N and Ce anomaly with La_N/Sm_N ratios >0.35 . The Gezhongwu phosphorites show no correlation between the two parameters (Fig. 4), revealing the Ce anomaly is a depositional seawater signature.

Shields and Stille (2001) have shown that later diagenetic processes produced a good correlation between Ce and Eu anomalies, a negative correlation between Ce anomaly and Dy_N/Sm_N , and a positive correlation between Ce anomaly and REE contents in phosphorites. These correlations do not appear in the Gezhongwu phosphorites (Figs. 4 and 5), suggesting that diagenetic effects on the REE patterns are limited. For these reasons, the Gezhongwu phosphorites probably reflect the depositional conditions.

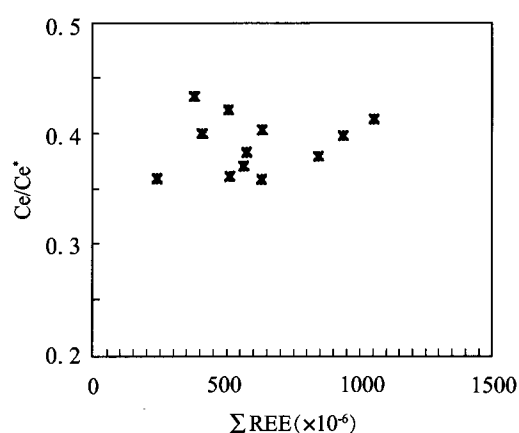


Fig. 5. Plot of Ce anomaly and the total REE abundance of the Gezhongwu phosphorites.

Wright et al. (1987) defined negative Ce anomalies as oxic conditions. The Gezhongwu phosphorites have a record of negative Ce anomalies. This suggests that marine depositional conditions are oxic.

Negative Ce anomalies of the Cambrian phosphorites collected from Zunyi, Guizhou Province and Kunyang, Yunnan Province are similar (Yang Weidong et al., 1997), suggesting that oxic seawater conditions prevailed in a vast area of Southwest China at the time Cambrian phosphorites were deposited.

5 Conclusions

Characteristic features pertaining to total abundances, elemental abundances and distribution patterns of the REE in the Gezhongwu Formation phosphorites are described. The total REE concentrations of the Gezhongwu phosphorites are higher than those of other Early Cambrian phosphorites, and the values of dolomitic and siliceous phosphorites are higher than those of phosphatic dolomite. Both the phosphorites are rich in yttrium. Hat-shaped patterns of the PAAS-normalized REE distribution preserved the primary signatures of seawater. Later diagenesis and weathering processes have only minimal effects on the Gezhongwu phosphorites. Seawater served as the immediate source of the REE in 'old' phosphorites, their characteristic depletion in HREE may be related to the evolutionary trend of the REE in seawater. Negative Ce anomalies in the Gezhongwu phosphorites suggest that the depositional conditions are oxic. The phosphorites are characterized by positive Eu anomaly, high Σ REE and hat-shaped REE pattern, suggesting that the Gezhongwu phosphorites were deposited in the normal marine environment mixed with hydrothermal water.

Acknowledgements The authors are grateful to Yan Jiabin (China University of Geoscience, Wuhan) and Li Xiaomin (University of Jilin, Changchun) for reviewing the earlier draft.

References

- Altschuler Z. S. (1980) The geochemistry of trace elements in marine phosphorite, 1. Characteristic abundance and enrichment. In *Marine Phosphorites* (ed. Y. K. Bendor) [C]. **29**, 19–30. SPEM Spec. Publ.
- Barfod G. H., Albarede F., Knoll A. H., Xiao S., Telouk P., Frei R., and Baker J. (2002) New Lu-Hf and Pb-Pb age constraints on the earliest animal fossils [J]. *Earth Planetary Science Letter*. **201**, 203–212.
- Bau M. (1991) Rare-earth element mobility during hydrothermal and metamorphic fluid-rock interaction and the significance of the oxidation state of europium [J]. *Chemical Geology*. **93**, 219–230.
- Bertram C. J., Elderfield H., Aldridge R. J., and Conway M. S. (1992) $^{87}Sr/^{86}Sr$, $^{143}Nd/^{144}Nd$ and REEs in Silurian phosphatic fossils [J]. *Earth Planetary Science Letter*. **113**, 239–249.
- Bertrand S. J., Flicoteaux R., Moussine P. A., and Ahmed A. A. K. (1997) Lower Cambrian apatitic stromatolites and phosphorites related to the glacio-eustatic cratonic rebound (Sahara, Algeria) [J].

- J. Sediment. Res.* **67**, 957–974.
- Bonnoit C. C. and Flicoteaux R. (1989) Distribution of rare-earth and some trace elements in Tertiary phosphorites from the Senegal Basin and their weathering products [J]. *Chemical Geology*. **75**, 311–328.
- Brookins D. G. (1989) Aqueous geochemistry of rare-earth elements. In *Geochemistry and Mineralogy of Rare Earth Elements* (eds. B. R. Lipin and G. A. McKay) [C]. Min. Soc. Am., Rev. Mineral. **21**, p. 221–225.
- Chen Duofu, Dong Weiquan, Qi Liang, Chen Guangqian, and Chen Xiapei (2003) Possible REE constrains on the depositional and diagenetic environment of Doushantuo Formation phosphorites containing the earliest metazoan fauna [J]. *Chemical Geology*. **201**, 102–118.
- Cook P. J. and Shergold J. H. (1984) Phosphorus, phosphorite and skeletal evolution at the Precambrian-Cambrian boundary [J]. *Nature*. **308**, 231–236.
- Elderfield H. and Sholkovitz E. R. (1987) Rare-earth elements in the pore waters of reducing nearshore sediments [J]. *Earth Planetary Science Letter*. **82**, 280–288.
- German C. R. and Elderfield H. (1990) Application of the Ce anomaly as a paleoredox indicator: The ground rules [J]. *Paleoceanography*. **5**, 823–833.
- Grandjean P., Cappetta H., Michard A., and Albarede F. (1987) The assessment of REEs patterns and $^{143}\text{Nd}/^{144}\text{Nd}$ ratio in fish remains [J]. *Earth Planetary Science Letter*. **84**, 181–196.
- Hannigan R. E. and Sholkovitz E. R. (2001) The development of middle rare-earth element enrichments in freshwaters: Weathering of phosphatic minerals [J]. *Chemical Geology*. **175**, 495–508.
- Haskin L. A. (1990) PREconceptions pREEvent pREEcise pREEdictions [J]. *Geochim. Cosmochim. Acta*. **54**, 2353–2361.
- Ilyin A. V. (1998) Rare-earth geochemistry of 'old' phosphorites and probability of syngenetic precipitation and accumulation of phosphate [J]. *Chemical Geology*. **144**, 243–256.
- Jarvis I., Burnett W., Nathan Y., Almbatydin F. S. M., Attia A. K. M., Castro L. N., Flicoteaux R., Hilmy M. E., Husain V., Qutawnah A. A., Serjani A., and Zanin Y. N. (1994) Phosphorite geochemistry state-of-the-art and environment concerns [J]. *Eclogae Geol. Helv.* **87**, 643–700.
- Lecuyer C., Grandjean P., Barrat J., Nolvak J., Emig C., and Paris F. (1998) ^{18}O and REE contents of phosphatic brachiopods: A comparison between modern and lower Paleozoic populations [J]. *Geochim. Cosmochim. Acta*. **62**, 2429–2436.
- Li Shengrong and Gao Zhenmin (1995) REE characteristics of black rock series of the lower Cambrian Niutitang Formation in Hunan-Guizhou provinces, China, with a discussion on the REE patterns in marine hydrothermal sediments [J]. *Acta Mineralogica Sinica*. **15**, 225–228.
- Mazumdar A., Banerjee D. M., Schidlowski M., and Balaram V. (1999) Rare-earth elements and stable isotope geochemistry of early Cambrian chert-phosphorite assemblages from the Lower tal Formation of the Krol Belt (lesser Himalaya, India) [J]. *Chemical Geology*. **156**, 275–297.
- McArthur J. M. and Walsh J. N. (1984) Rare-earth geochemistry of phosphorites [J]. *Chemical Geology*. **47**, 191–220.
- McLennan S. M. (1989) Rare-earth elements in sedimentary rocks: influence of provenance and sedimentary processes. In *Geochemistry and Mineralogy of Rare-Earth Elements* (eds. B. R. Lipin and G. A. McKay) [C]. Min. Soc. Am. Rev. Mineral. **21**, 169–200.
- Michard A. and Albarede F. (1986) The REE content of some hydrothermal fluids [J]. *Chemical Geology*. **55**, 51–60.
- Morad S. and Felitsyn S. (2001) Identification of primary Ce-anomaly signatures in fossil biogenic apatite: Implication for the Cambrian oceanic anoxia and phosphogenesis [J]. *Sedimentary Geology*. **143**, 259–264.
- Murray R. W., Buchholtz M. R., Gerlach D. C., Russ G. P. III, and Jones D. L. (1992) Rare-earth, major, and trace element composition of Monterey and DSDP chert and associated host sediments: Assessing the influence of chemical fractionation during diagenesis [J]. *Geochim. Cosmochim. Acta*. **56**, 2657–2671.
- Olivarez A. M. and Owen R. M. (1991) The europium anomaly of seawater: Implications for fluvial versus hydrothermal REE inputs to the oceans [J]. *Chemical Geology*. **92**, 317–328.
- Picard S., Lecuyer C., Barrat J., Garciaud J., Dromart G., and Sheppard S. M. F. (2002) Rare-earth element contents of Jurassic fish and reptile teeth and their potential relation to seawater composition (Anglo-Paris Basin, France and England) [J]. *Chemical Geology*. **186**, 1–16.
- Qi Liang and Gregoire D. C. (2000) Determination of trace elements in 26 Chinese geochemistry reference materials by inductively coupled plasma mass spectrometry [J]. *Geostand. Newsl.* **24**, 51–63.
- Reynard B., Lecuyer C., and Grandjean P. (1999) Crystal-chemical controls on rare-earth element concentrations in fossil biogenic apatites and implications for paleoenvironmental reconstructions [J]. *Chemical Geology*. **155**, 233–241.
- Shields G. and Stille P. (2001) Diagenetic constrains on the use of cerium anomalies as palaeoseawater redox proxies: An isotopic and REE study of Cambrian phosphorites [J]. *Chemical Geology*. **175**, 29–48.
- Sverjensky D. A. (1984) Europium redox equilibria in aqueous solution [J]. *Earth Planet Sci. Lett.* **67**, 70–78.
- Wright J., Schrader H., and Holser W. T. (1987) Paleoredox variations in ancient oceans recorded by rare-earth elements in fossil apatite [J]. *Geochim. Cosmochim. Acta*. **51**, 637–644.
- Yang Jiedong and Sun Weiguo (1999) Variations in Sr and C isotopes and Ce anomalies in successions from China: evidence for the oxygenation of Neoproterozoic seawater [J]. *Precambrian Research*. **93**, 215–233.
- Yang Weidong and Qi Liang (1995) The geochemistry characteristic and genesis of REE of the phosphorites rock series in earlier Cambrian, in eastern Yunnan [J]. *Bulletin of Mineralogy, Petrology and Geochemistry*. **12**, 224–227.
- Yang Weidong, Xiao Jinkai, Yu Binshong, Fang Tao, Chen Feng, and Lu Xiaoyin (1997) *Sedimentology and Geochemistry of Phosphorites in Southwest of China* [M]. pp. 105. Science Press, Beijing (in Chinese).
- Yang Yaomin, Tu Guangzhi, and Hu Ruizhong (2004) REE and trace element geochemistry of Yinachang Fe-Cu-REE deposit, Yunnan Province, China [J]. *Chinese Journal of Geochemistry*. **23**, 265–274.